Performance analysis of a plate heat exchanger using various nanofluids

Zheng, Dan; Wang, Jin; Chen, Zhanxiu; Baleta, Jakov; Sundén, Bengt

International Journal of Heat and Mass Transfer 158 (2020) 119993

Contents lists available at ScienceDirect

International Journal of Heat and Mass Transfer

journal homepage: www.elsevier.com/locate/hmt

Performance analysis of a plate heat exchanger using various nanofluids

Dan Zheng[a], Jin Wang[a,*], Zhanxiu Chen[a], Jakov Baleta[b], Bengt Sundén[c,*]

[a] School of Energy and Environmental Engineering, Hebei University of Technology, Tianjin 300401, China
[b] Faculty of Metallurgy, University of Zagreb, Sisak 44000, Croatia
[c] Department of Energy Sciences, Division of Heat Transfer, Lund University, P.O. Box 118, Lund, SE-22100, Sweden

ARTICLE INFO

Article history:
Received 16 March 2020
Revised 3 May 2020
Accepted 24 May 2020
Available online 30 June 2020

Keywords:
Nanofluid
Heat transfer enhancement
Pressure drop
Empirical formula
Plate heat exchanger

ABSTRACT

In this paper, a corrugated plate heat exchanger in solar energy systems is used to investigate heat transfer and fluid flow characteristics of various nanofluids. By adding various nanoparticles (Al_2O_3-30 nm, SiC-40 nm, CuO-30 nm and Fe_3O_4-25 nm) into the base fluid, effects of nanofluid types and particle concentrations (0.05 wt.%, 0.1 wt.%, 0.5 wt.% and 1.0 wt.%) on the thermal performance of the plate heat exchanger are analyzed at flow rates in the range of 3–9 L/min. Results indicate that both heat transfer enhancement and pressure drop for nanofluids show significant increases compared to the base fluid. The Fe_3O_4-water and CuO-water nanofluids show the best and the worst thermal performances of the plate heat exchanger, respectively. When 1.0 wt.% Fe_3O_4-water nanofluid is used as the working fluid, compared to DI-water, the convective heat transfer coefficient is increased by 21.9%. However, an increase of 10.1% in pressure drop is obtained for the 1.0 wt.% Fe_3O_4-water nanofluid. Finally, empirical formulas of experimental Nusselt number are obtained based on the experimental data. A new way to predict the thermal performance for various nanofluids in heat transfer systems is provided.

1. Introduction

Solar energy has become an important part of sustainable energy to solve problems of fossil fuel shortages and serious environmental pollution. Developing new solar energy technologies and improving the utilization are research focuses at present. Nanofluids are high-efficient heat transfer media, and numerous studies have proven that thermal conductivities of nanofluids are higher than those of conventional fluids (such as water, oil and ethylene glycol) [1].

Nowadays, nanofluids have been widely used in solar energy systems, heat exchangers, automobile radiators, electronic chips, etc. However, especially in a solar energy system, nanofluids have a great potential [2], some practical limitations and enormous challenges [3]. Michael and Iniyan [4] improved the thermal performance of photovoltaic thermal collectors using CuO-water nanofluids. They found that the thermal efficiency increased up to 45.76% for a CuO-water nanofluid with 0.05% volume fraction, compared to water at a mass flow rate of 0.01 kg/s. Chen et al. [5] pointed out that the solar-thermal conversion efficiency increased with the increase in the nanoparticle concentration of multi-walled carbon nanotubes (MWCNTs). They found that 0.01 wt.% MWCNTs nanofluid with a fluid thickness above 0.5 cm could absorb nearly all the incident energy. Yurddaş [6] numerically conducted a comparison of the thermal performance for various nanofluids in an evacuated tube solar collector. It was found that the outlet temperature of the water tank increased by 14.09% for 5 vol.% Cu-water nanofluid compared to water. Abbas et al. [7] presented improvement in photovoltaic thermal (PV/T) systems. They found that a volume fraction of nanoparticle concentration below 5% was appropriate to avoid a clustering process of nanoparticles. Radwan and Ahmed [8] developed a new method to cool concentrating photovoltaic systems by using a wide microchannel heat sink with nanofluids (SiC-water and Al_2O_3-water nanofluids). They found that the cell electrical efficiency increased by 14% for a 4% SiC-water nanofluid at *Re*=12.5. Mercan and Yurddaş [9] both experimentally and numerically analyzed the effects of various factors (type of nanofluid, volume fraction of nanoparticles, collector angle, mass flow rate and number of evacuated tubes) on the heat transfer characteristics of evacuated tube solar collectors. They found that when the volume fraction is 5% and the number of tubes is 24, the tank outlet temperature increased

* Corresponding authors.
E-mail addresses: zhanxiu_chen@hebut.edu.cn (Z. Chen), baleta@simet.hr (J. Baleta), bengt.sunden@energy.lth.se (B. Sundén).

https://doi.org/10.1016/j.ijheatmasstransfer.2020.119993

NOMENCLATURE

A	total heat transfer area, m^2
c_p	specific heat, J $kg^{-1}K^{-1}$
h	convective heat transfer coefficient, W m^{-2} K^{-1}
L	plate length, mm
N	number of corrugated plates
Nu	Nusselt number
P	pressure, Pa
Pr	Prandtl number
Q	heat transfer rate, W
Re	Reynolds number
t	corrugation pitch, mm
U	overall heat transfer coefficient, $Wm^{-2}K^{-1}$
V	volume flow rate, L min^{-1}
W	plant width, mm

Greek symbols

β	corrugation angle,
δ	plate thickness, mm
φ	volume concentration, vol.%
λ	thermal conductivity, W m^{-1} K^{-1}
μ	dynamic viscosity, Pa s
ρ	density, kg m^{-3}
ω	mass fraction of nanoparticles, wt.%

Subscripts

ave	average
c	cold
d	dispersant
h	hot
in	inlet
nf	nanofluid
out	outlet
p	particle
w	water

Abbreviation

LMTD	logarithmic mean temperature difference, K

by 4.13% and 6.80% for Al_2O_3-water and CuO-water nanofluids, respectively.

In order to widen the application range of nanofluids, a mixture of water and ethylene glycol is often used as the base fluid to prepare the nanofluid. Xu et al. [10] investigated the physical properties of water-ethylene glycol based graphene oxide nanofluid to improve the photo-thermal conversion performance of a direct absorption solar collector. Compared with the base fluid, the efficiency of the receiver increased by 70% with 240 s irradiation duration when this nanofluid was used. They found that the graphene oxide nanofluid showed a great potential for practical applications. Hashimoto et al. [11] proposed a correlation formula between the Nusselt number and the Reynolds number for the SiO_2 nanofluid. It was found that the 50 wt.% SiO_2-ethylene glycol/water nanofluid showed up to 25% increase in heat transfer performance, compared to the ethylene glycol/water solution. The water-ethylene glycol based ZnO nanofluid was used as the working fluid in a flat plate solar collector by Choudhary et al. [12]. A 70.28% thermal efficiency for 1.0 vol.% ZnO nanofluid was obtained at a flow rate of 90 L/h. Based on a mixture of ethylene glycol and water (EGW), the thermal performance of nanofluids in an indoor electric heater was investigated by Chen et al. [13]. They found that the heating performance increased by 14.7% using 0.5% Fe_3O_4-EGW nanofluid under a magnetic field of 100 mT. Convective heat transfer characteristics of ferrofluids inside a pipe with various external magnetic fields were investigated by Wang et al. [14]. They found that 261% enhancement on heat transfer was obtained using five adjacent magnetic cannulas at high Reynolds number.

Nanofluids are also used as coolants to cool devices and improve the operation stability. Based on a mixture of distilled water (DW) and ethylene glycol (EG), Said et al. [15] carried out an investigation of the heat transfer performance of Al_2O_3 and TiO_2 nanofluids in an actual automobile radiator. They found that the most stable sample from 0.3 vol.% Al_2O_3-DW/EG nanofluids with 1:1 mass ratio of nanoparticles to Arabic gum (AG) surfactant was the most stable nanofluid within the range of the tests. Devireddy et al. [16] improved the performance of automobile radiators using glycol solution based TiO_2 nanofluids, and the 0.3 vol.% TiO_2-DW/EG nanofluid resulted in a heat transfer enhancement of 35%. Nagarajan et al. [17] investigated thermophysical properties of an alumina-silica hybrid nanocoolant, and they found that the overall heat transfer coefficient of a jacketed vessel filled with this hybrid nanocoolant increased by 52.8% compared to conventional coolant. Al-Rashed et al. [18] both experimentally and numerically studied the performance of heat sinks for CPU cooling using CuO-water nanofluids. They concluded that by using 2.25 vol.% CuO nanofluid, 7.7% improvement of the thermal conductivity was obtained at a heat load of 115 W at a Reynolds number of 1100. Kumar and Kumar [19] numerically studied heat transfer characteristics of Al_2O_3-water nanofluids in six circular channel heat sinks to cool electronic chips. They found that increments of 12%, 26%, and 40% in the heat transfer coefficient were obtained for 0.25%, 0.5%, and 0.75% Al_2O_3-water nanofluids compared to water, respectively.

The energy conversion rate of solar energy systems is improved, when nanofluids are used in the heat exchangers. Recent applications of nanofluids in heat exchangers were reviewed by Pordanjani et al. [20]. Heat transfer enhancements of non-Newtonian nanofluids (like aqueous carboxymethyl cellulose based Fe_2O_3, Al_2O_3 and CuO nanofluids) in a shell and helical coil heat exchanger were experimentally investigated by Naik and Vinod [21]. Results revealed that the overall heat transfer coefficient of the CuO nanofluid had a maximum enhancement of 29% for a mass concentration of 1%. Li et al. [22] investigated heat transfer and fluid flow characteristics of carbon-acetone nanofluids in a microchannel heat sink. They pointed out that about 73% enhancement in the heat transfer coefficient was found when 0.1 wt.% carbon-acetone nanofluid was used as the working fluid. Qi et al. [23] analyzed pressure drops and heat transfer characteristics of TiO_2-water nanofluids in corrugated double-tube heat exchangers. Compared with deionized water in the corrugated double-tube heat exchanger, heat transfer rates of TiO_2-water nanofluids with mass fractions of 0.1%, 0.3%, and 0.5% increased by 10.8%, 13.4% and 14.8%, respectively. Mazaheri et al. [24] analyzed the entropy generation and exergy destruction of a graphene nanoplatelets nanofluid in a ribbed triple-tube heat exchanger (RTTHX). It was observed that the total exergy destruction of the whole RTTHX was reduced when the nanoparticle mass fraction increased. Kumar and Chandrasekar [25] analyzed heat transfer characteristics of double helically coiled tube heat exchangers with MWCNT-water nanofluids based on a comparison of the Dean Number. It was found that for a 0.6 vol.% nanofluid, the Nusselt number and pressure drop increased by 30% and 10% at a Dean number of 2000, respectively. Radkar et al. [26] investigated convective heat transfer characteristics of helical copper tube heat exchangers under a constant wall temperature condition. They found that the average Nusselt number increased by 18.6% for 0.25 vol.% ZnO nanofluid. Bianco et al. [27] numerically investigated the heat transfer performance of an asymmetric heated channel filled with Al_2O_3-water nanofluid. The increase of the Nusselt number was 15% for the 6% Al_2O_3-water nanofluid at a Reynolds num-

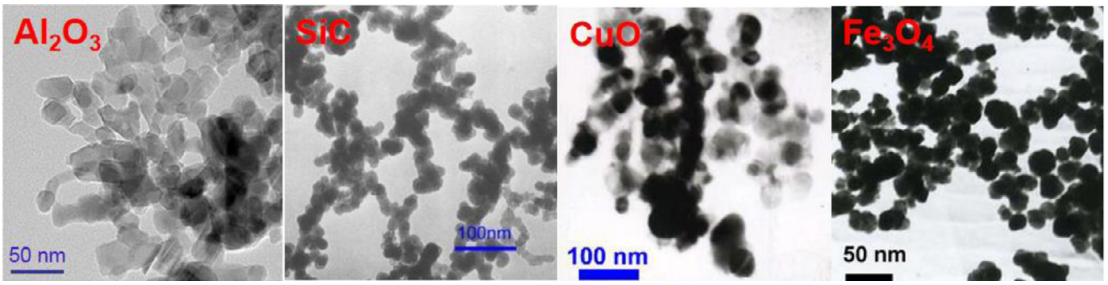

Fig. 1. Scanning electron microscope (SEM) images of various nanoparticles.

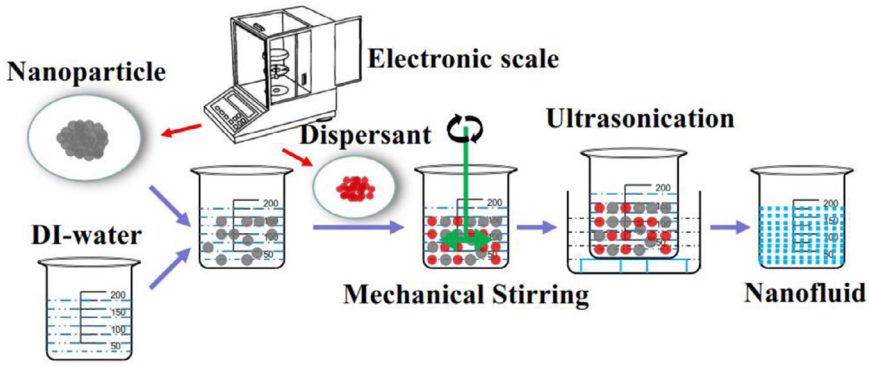

Fig. 2. Process of nanofluid preparation.

Table 1
Thermophysical properties of nanoparticles and deionized water (25 °C).

Material	Particle morphology	Particle size (nm)	Density (kg/m^3)	Specific heat (J/kg K)	Thermal conductivity (W/m K)
DI-water	/	/	997	4180	0.613
Al_2O_3	Spherical	30	3900	880	42.34
SiC	Nearly spherical	40	3370	1340	150
CuO	Nearly spherical	30	6500	540	18
Fe_3O_4	Spherical	25	5180	670	80

ber of 1000. Huang et al. [28] investigated thermal performance of Al_2O_3 and Al_2O_3−MWCNT hybrid nanofluids in a chevron plate heat exchanger. They proposed a correlation to predict all the experimental data within an error band of ±10%. Bhattad et al. [29] pointed out that increasing the volume ratio of MWCNT nanoparticles in an Al_2O_3−MWCNT hybrid nanofluid was beneficial for the performance improvement of the plate heat exchangers. Shirzad et al. [30] numerically investigated heat transfer characteristics and pressure drops of a pillow plate heat exchanger with various nanofluids. Results showed that compared to water at Re = 1000, the thermal performance of 5 vol.% Al_2O_3-water nanofluid showed an improvement of 43.4%.

In most cases, it is proved that addition of nanoparticles into a base fluid usually improve the thermal performance of industrial equipment. However, only few studies have been conducted to compare heat transfer enhancements of various nanofluids in heat exchangers at a large range of the mass flow rate. Generally, there were only few types of nanofluids investigated in the plate heat exchangers in previous studies. This paper aims to investigate the thermal performance of various nanofluids in a plate heat exchanger, including CuO-water, SiC-water, Al_2O_3-water and Fe_3O_4-water nanofluids. A new empirical formula with a high prediction accuracy is proposed based on the present experimental data. Finally, the nanofluid with the optimal heat transfer performance is recommended for solar energy systems.

2. Experimental investigation

2.1. Preparation of nanofluids

The nanoparticles, i.e., Al_2O_3, SiC, CuO and Fe_3O_4, used in this work were purchased from the Deke Daojin Company (China) and the scanning electron microscope (SEM) images of these nanoparticles are shown in Fig. 1. This company provided information of particle size, shape, and purity. Physical parameters of both nanoparticles and deionized water are listed in Table 1.

Nanoparticles were first dispersed into the DI-water by mechanical stirring, and then ultrasonic vibration was used to further improve the dispersible homogeneity. In order to improve the nanofluid stability, suitable dispersants are added into the mixed fluid with various nanoparticle mass fractions (0.05 wt.%, 0.1 wt.%, 0.5 wt.% and 1.0 wt.%) as shown in Fig. 2. Different dispersants are chosen to prepare different nanofluids due to various surface properties of the nanoparticles. Considering ultrasonication time and dispersant dosage, information of the nanofluid prepara-

Table 2
Details of nanofluid preparation.

Nanofluid	Mechanical stirring time	Ultrasonication time	Dispersant	$Mass_p$: $Mass_d$
Al_2O_3-water	30 min	1 h	Sodium hexametaphosphate	4:1
SiC-water	40 min	2 h	Cetyltrimethylammonium bromide	5:3
CuO-water	30 min	1.5 h	Sodium hexametaphosphate	4:1
Fe_3O_4-water	30 min	1 h	Sodium citrate	5:1

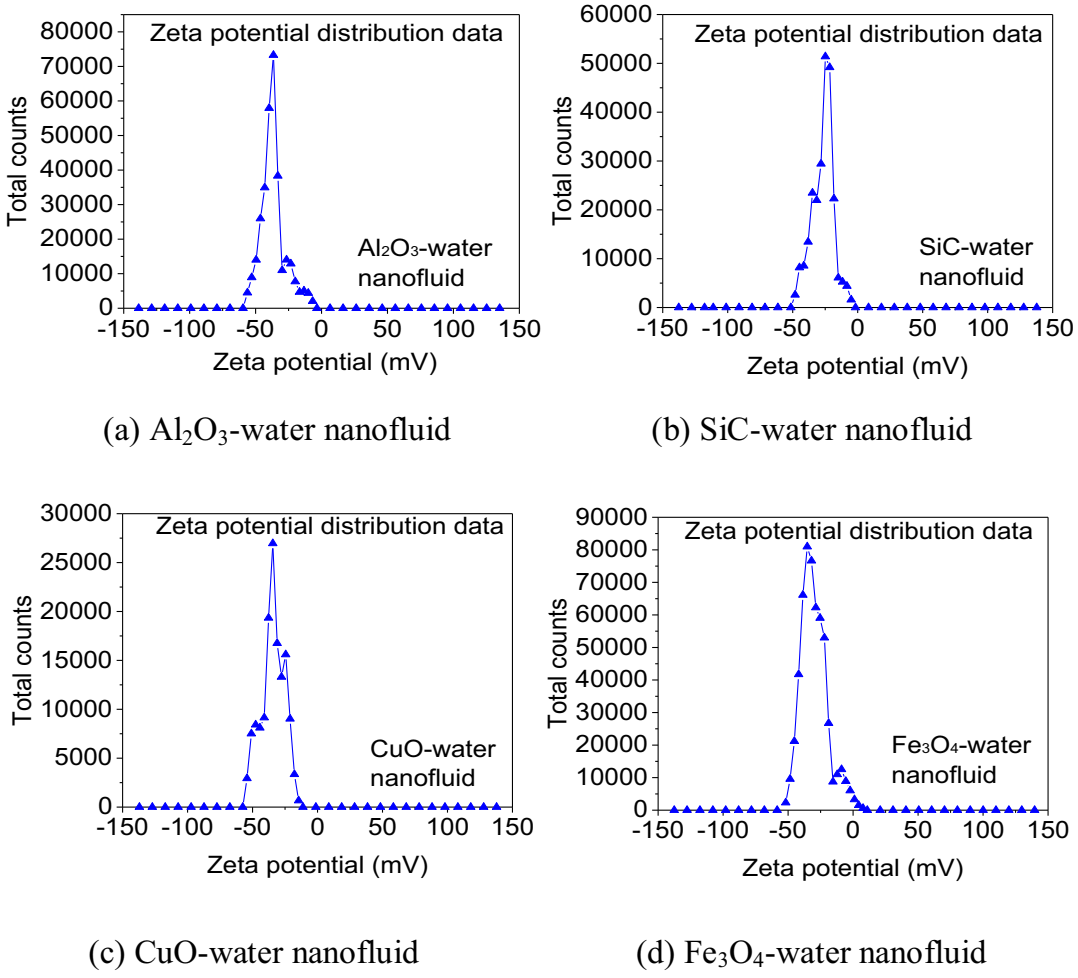

Fig. 3. Zeta (ζ) potential distribution of nanofluids.

tion process is shown in Table 2. In this table, the value of $Mass_p$: $Mass_d$ means the mass ratio of particle and dispersant.

Fig. 3 shows zeta (ζ) potential distributions for all four nanofluids with a mass fraction of 1.0 wt.%. In this research, the values of the zeta (ζ) potential for the nanofluids were measured by the Zetasizer Nano ZS90 with an accuracy of 0.12 μm•cm/V•s. Zeta (ζ) potential is an important index to characterize the stability of colloidal dispersion nanofluids. For a stable fluid, the nanoparticles with a lot of positive and negative charges in the liquid will repel each other, which results in high zeta potential. For a nanofluid, a high absolute value of the zeta (ζ) potential corresponds to high stability of the colloidal dispersion. Usually, the colloidal dispersion of the nanofluid shows a better stability with a zeta (ζ) potential above 25. It is found that values of the zeta ζ potential for Al_2O_3-water, SiC-water, CuO-water and Fe_3O_4-water nanofluids are −36.7 mV, −26.8 mV, −34.5 mV and −29.9 mV, respectively. Results indicate that the prepared nanofluids have good stability.

2.2. Experimental setup

The present experimental setup consists of two flow loops, i.e., a water loop and a nanofluid loop. In Fig. 4, the right loop represents the flowing circulation of the hot water, and the left loop represents the flowing circulation of the nanofluid. Thermocouples are arranged at the inlet and outlet of the plate heat exchanger to measure the fluid temperatures. The inlet temperatures of nanofluid and hot water are maintained at 27±1 °C and 50±1 °C, respectively. The pressure drop of the nanofluid through the corrugated plate heat exchanger is measured by a differential pressure gauge.

Fig. 5 shows a schematic of the heat exchanger and corrugated plate. The length and width of the plate heat exchanger are 170 mm and 70 mm, respectively. The plate heat exchanger is composed of 28 corrugated plates with an average thickness of 0.5 mm. Other geometrical dimensions of the corrugated plate heat exchanger are shown in Table 3.

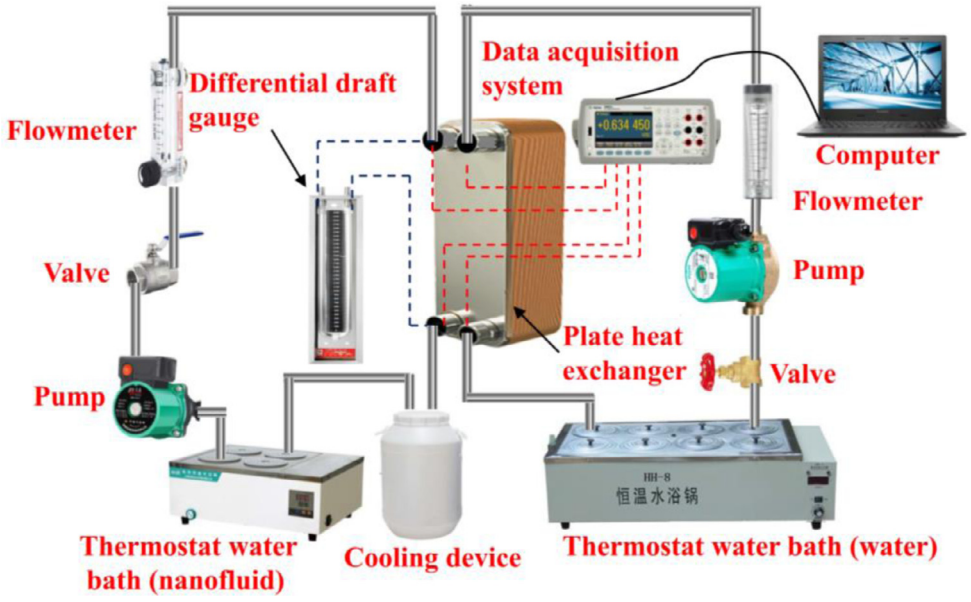

Fig. 4. Schematic of the experimental system.

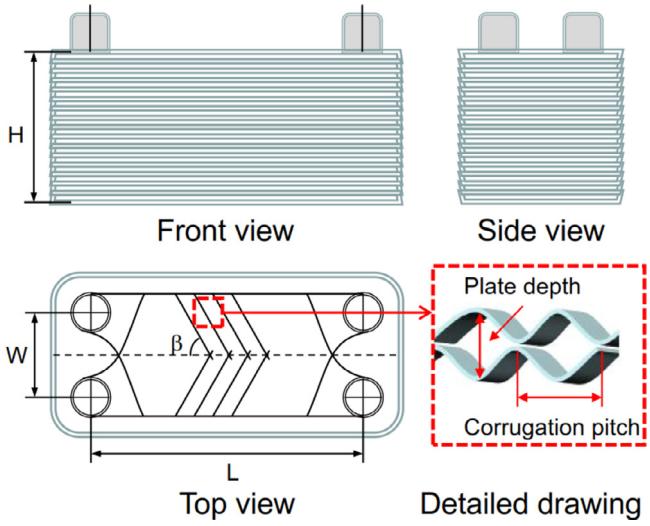

Fig. 5. Schematic of the heat exchanger and corrugated plate.

Table 3
Geometrical dimensions of the corrugated plate heat exchanger.

Parameters	Value
Corrugation angle, β	60°
Corrugation pitch, t	9 mm
Number of corrugated plate, N	28
Plate length, L	170 mm
Plant width, W	70 mm
Plate depth, $2b_c$	4.8 mm
Plate thickness, δ	0.5 mm
Total heat transfer area, A	0.378 m^2
Surface enlargement ratio	1.13

2.3. Data analysis

In theory, the released heat from the hot fluid is equal to the absorbed heat from the cold fluid in a heat exchanger, and the heat amount for the hot fluid and cold fluid can be calculated by Eqs. (1) and (2), respectively. Q_{ave} represents the average heat power of the hot fluid and the cold fluid and is calculated by Eq. (3)

$$Q_h = m_h C_{p,h}(T_{h,in} - T_{h,out}) \quad (1)$$

$$Q_c = m_c C_{p,c}(T_{c,out} - T_{c,in}) \quad (2)$$

$$Q_{ave} = (Q_h + Q_c)/2 \quad (3)$$

The overall heat transfer coefficient (U) can be calculated by Eq. (4)

$$U = \frac{Q_{ave}}{A \cdot LMTD} \quad (4)$$

where A represents the total heat transfer area (0.378 m^2). $LMTD$ represents the logarithmic mean temperature difference from Eq. (5). The expression for $LMTD$ calculation in this paper is given in Eq. (6):

$$LMTD = \frac{\Delta t_{\max} - \Delta t_{\min}}{\ln \frac{\Delta t_{\max}}{\Delta t_{\min}}} \quad (5)$$

$$LMTD = \frac{(T_{h,out} - T_{c,in}) - (T_{h,in} - T_{c,out})}{\ln \frac{(T_{h,out} - T_{c,in})}{(T_{h,in} - T_{c,out})}} \quad (6)$$

The heat transfer coefficient of the nanofluid (h_{nf}) can be calculated using Eq. (7):

$$\frac{1}{U} = \frac{1}{h_{nf}} + \frac{\delta}{\lambda} + \frac{1}{h_w} \quad (7)$$

where δ and λ represent the width and thermal conductivity of the corrugated plate, respectively. h_w is the convective heat transfer coefficient of the water. In this work, the heat transfer performance of the hot water was obtained by using the following equation [31]:

$$Nu = 1.615[(fRe/64)RePrD/L]^{1/3} \quad (8)$$

where Nu, Re, and Pr are Nusselt number, Reynolds number and Prandtl number, respectively. f is related to the flow characteristics and structure of the corrugated plate. D is the equivalent diameter, i.e., the plate depth for this work. The Reynolds number (Re) and Prandtl number (Pr) can be calculated by the following equations.

$$Re = \frac{\rho \upsilon D}{\mu} \quad (9)$$

Table 4
Typical models for predicting thermal conductivity.

Authors	Thermal conductivity	Viscosity
Maxwell [34]	$\frac{k_{nf}}{k_w} = \frac{k_p+2k_w+2\varphi(k_p-k_w)}{k_p+2k_w-\varphi(k_p-k_w)}$	/
Bruggeman [35]	$\varphi(\frac{k_p-k_{nf}}{k_p+2k_{nf}}) + (1-\varphi)(\frac{k_f-k_{nf}}{k_f+2k_{nf}}) = 0$	/
Einstein [36]	/	$\mu_{nf} = \mu_w(1+2.5\varphi)$
Brinkman [37]	/	$\mu_{nf} = \mu_w(1-2.5\varphi+1.552\varphi)^{-1}$

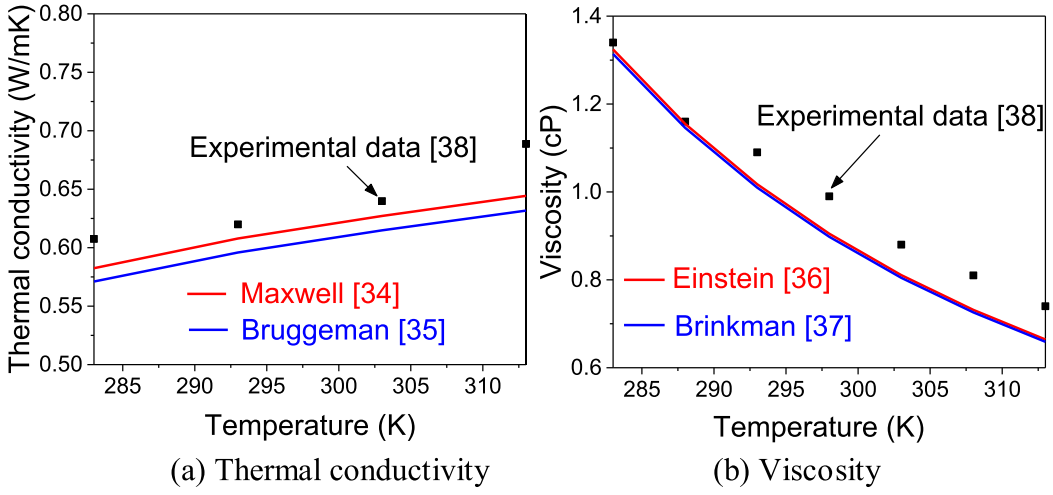

Fig. 6. Comparisons between measured results and theoretical calculated values for the thermal conductivity and viscosity of 0.5 vol.% Fe_3O_4-water nanofluid.

$$Pr = \frac{\mu C_p}{k} \tag{10}$$

It is obvious that the two dimensionless numbers are closely related to the fluid physical properties, such as density (ρ), flow velocity (v), viscosity (μ) and thermal conductivity (k). The Nusselt number of the hot water can be calculated as follows:

$$Nu = \frac{hD}{k} \tag{11}$$

Based on Eqs. (8) and (11), the heat transfer performance of the nanofluid was obtained.

2.4. Thermophysical properties of the nanofluid

In this paper, density and specific heat of the nanofluid are calculated as suggested in Refs. [32, 33]:

$$\rho_{nf} = (1-\varphi)\rho_w + \varphi\rho_p \tag{12}$$

$$(\rho c_p)_{nf} = (1-\varphi)(\rho c_p)_w + \varphi(\rho c_p)_p \tag{13}$$

where φ represents the volume fraction of the nanofluid. The subscripts *nf*, *w* and *p* represent nanofluid, water and particle, respectively.

The thermal conductivity was measured by the DRE-2B thermal property analyzer (Xiangtan Instrument & Meter Ltd., China) with an accuracy of ±3.0%, and the viscosity was measured by a brookfield DV2T viscosimeter (Brookfield Engineering Laboratories Company, USA) with an accuracy of ±1.0%. Many classical models in Refs. [34-37] were developed to calculate the thermal conductivity and viscosity of nanofluids as shown in Table 4.

For the thermal conductivity and viscosity of the 0.5 vol.% Fe_3O_4-water nanofluid, comparisons of measured results and theoretical calculated values have been conducted as shown in Fig. 6. It is found that the results from the theoretical calculations differ to some extent from the measured values. The main reasons are that the effects of dispersant and nanoparticle size have not been considered in these published classical models. More discussions on thermophysical properties of nanofluids can be found in the previous research [38], and specific empirical formulas for the thermal conductivity and viscosity of the Fe_3O_4-water nanofluid have been proposed.

Table 5
Uncertainties of measurements.

Measurements	Uncertainty
Temperature	± 0.1 K
Diameter	± 0.05 mm
Length	± 0.5 mm
Width	± 0.5 mm
Mass of nanoparticles	± 0.001 g
Volume flow	± 2.5%
Pressure drop, Δp	± 2%
Heat flow, Q	± 1.25%
Heat transfer coefficient, *h*	± 1.77%
Reynolds number, *Re*	± 3.71%
Nusselt number, *Nu*	± 3.59%

2.5. Analysis of uncertainties

The heat transfer performance of the corrugated plate heat exchanger filled with nanofluids is investigated by changing some parameters, such as inlet temperature, inlet flow rate, nanoparticle mass fraction, etc. Uncertainties of the tested and calculated values are listed in Table 5. An analysis of the experimental uncertainty is conducted based on the method presented in Moffat [39]:

$$\delta R = \left\{ \sum_{i=1}^{N} \left(\frac{\partial R}{\partial X_i} \delta X_i \right)^2 \right\}^{1/2} \tag{14}$$

where the variable R is a function of parameters X_1, X_2, ..., X_n, and δX_1, δX_2, ...δX_n are corresponding uncertainties of these parameters. Uncertainties of Reynolds number, heat flow, heat transfer coefficient and Nusselt number can be calculated by applying

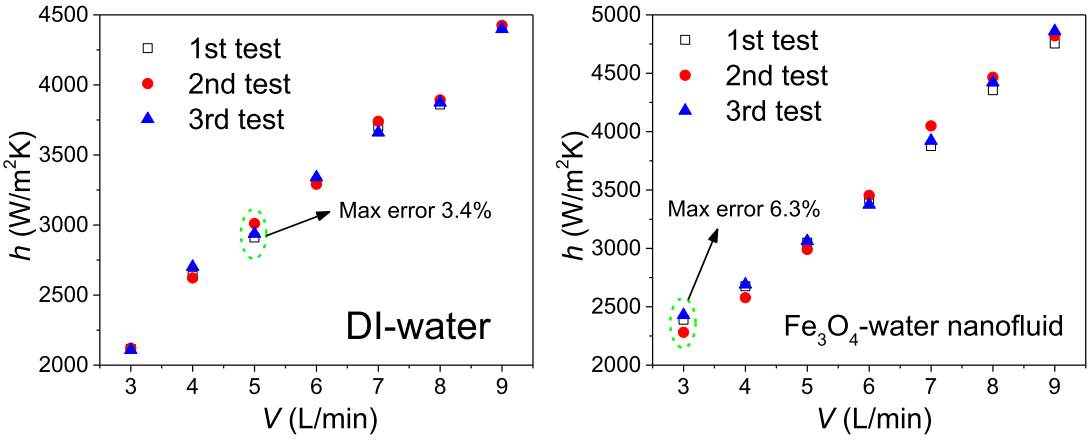

(a) DI-water (b) Fe_3O_4-water nanofluid

Fig. 7. Repeatability validation of experimental results.

Eqs. (15-18):

$$\delta Re = \sqrt{\left(\frac{\Delta\rho}{\rho}\right)^2 + \left(\frac{\Delta\mu}{\mu}\right)^2 + \left(\frac{\Delta\upsilon}{\upsilon}\right)^2 + \left(\frac{\Delta D}{D}\right)^2} \quad (15)$$

$$\delta Q = \sqrt{\left(\frac{\Delta m}{m}\right)^2 + \left(\frac{\Delta C_p}{C_p}\right)^2 + \left(\frac{\Delta T}{T}\right)^2} \quad (16)$$

$$\delta h = \sqrt{\left(\frac{\Delta A}{A}\right)^2 + \left(\frac{\Delta Q}{Q}\right)^2 + \left(\frac{\Delta T}{T}\right)^2} \quad (17)$$

$$\delta Nu = \sqrt{\left(\frac{\Delta h}{h}\right)^2 + \left(\frac{\Delta k}{k}\right)^2 + \left(\frac{\Delta D}{D}\right)^2} \quad (18)$$

3. Results and discussion

The heat transfer performance and pressure drop of the plate heat exchanger with nanofluids are discussed in this section. Finally, new empirical formulas of experimental *Nu* values are proposed.

3.1. Repeatability test

Every measurement for the nanofluid was conducted at least three times to reduce errors of the experimental results. Fig. 7 shows a repeatability investigation on the experimental results for the DI-water and 0.05 wt.% Fe_3O_4-water nanofluid. The maximum differences are 3.4% and 6.3% for DI-water and Fe_3O_4-water nanofluid, respectively. This result indicates that a good consistency in the heat transfer coefficient is obtained during three tests.

3.2. Heat transfer performance

Heat transfer performance of the various nanofluids are depicted in Fig. 8 and analyzed at different volume flow rates (3 L/min, 6 L/min and 9 L/min). Compared to DI-water at a volume flow rate of 9 L/min, the overall heat transfer coefficients increase by 6.0%, 4.8%, 4.9% and 5.9% for the 0.5 wt.% Fe_3O_4-water, CuO-water, Al_2O_3-water and SiC-water nanofluids, respectively. A comparison of the overall heat transfer coefficients at all tested flow rates (3 L/min, 6 L/min and 9 L/min) shows that the maximum increment of 9.4% is obtained for 1.0 wt.% Al_2O_3-water nanofluid, whereas the minimum increment of 0.6% is observed for 0.05 wt.% SiC-water nanofluid. Thus, it is concluded that the overall heat transfer coefficient increases with an increase in the volume flow rate. This is so because the increase in the volume flow rate results in more intensive nanoparticle movements and larger velocity difference between the particle and the base fluid. In addition, the supply of nanoparticles improves the thermal conductivity of the base fluid, and the thermal conductivity of the nanofluid increases with the increase in the nanoparticle concentration. However, even for the same nanofluid, increasing the flow rate may lead to a reduction of the heat transfer enhancement compared to DI-water. For 0.1 wt.% Fe_3O_4-water nanofluid, a flow rate increase from 3 L/min to 6 L/min results in 2.6% reduction of heat transfer enhancement (from 9.3% to 6.7%). This result is because the high concentration will result in higher viscosity. Therefore, the observed results are obtained based on the interaction of various factors, including nanoparticle movement, thermal conductivity and viscosity of the nanofluid.

Fig. 9 shows the variation trends of the heat transfer coefficients of the various nanofluids at different flow rates. It is found that the convective heat transfer coefficient of the nanofluid is higher than that of DI-water. Results indicate that the CuO-water nanofluid mostly shows better heat transfer performance than the others at a low particle concentration of 0.05 wt.%, whereas the Fe_3O_4-water nanofluid has generally higher performance compared to the other nanofluids at a nanoparticle particle concentration above 0.05 wt.%. At the same particle concentration of 1.0 wt.%, the heat transfer coefficients for Fe_3O_4-water, CuO-water, Al_2O_3-water and SiC-water nanofluids on average increase by 21.9%, 11.4%, 19.8% and 15.0%, respectively. For a mass fraction of 1.0 wt.% at 8 L/min, the Fe_3O_4-water nanofluid has the maximum increase of 30.8% of the convective heat transfer coefficient. Due to the high flow rate, the velocity increase of the particle movement decreases the thickness of the thermal boundary layer. These all contribute to the increase in the heat transfer performance of the plate heat exchanger. Based on the discussions of Figs. 8-9, it is concluded that the Fe_3O_4-water with higher than 0.05 wt.% mass fraction should be recommended for a good heat transfer performance of a plate heat exchanger.

3.3. Pressure drop (Δp)

Fig. 10 shows the relationship between the pressure drop and the volume flow rate for the four nanofluids with the optimum concentrations (1.0 wt.% Al_2O_3-water, 0.5 wt.% SiC-water, 0.5 wt.%

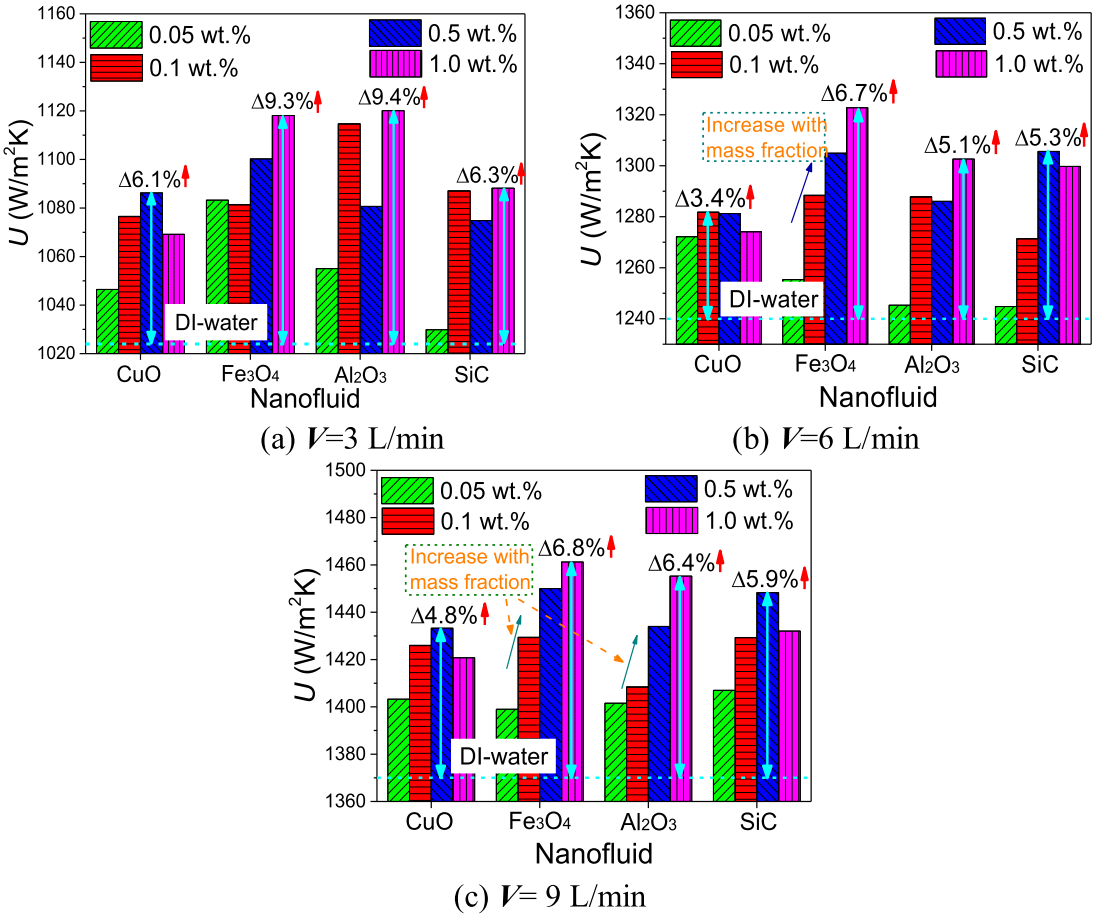

Fig. 8. Overall heat transfer coefficients versus volume flow rate.

CuO-water, and 1.0 wt.% Fe_3O_4-water nanofluids). It is found that the pressure drop of all the four nanofluids are higher than that of DI-water, and the pressure drop increases with the inlet flow rate. A high particle concentration is likely to promote aggregation and sedimentation of particles. These all cause an increase in the pressure drop. Compared with DI-water, the average pressure drops for the 0.5 wt.% SiC-water and 0.5 wt.% CuO-water nanofluids increase by 7.2% and 9.5%, respectively. The 1.0 wt.% Al_2O_3-water and Fe_3O_4-water nanofluids show somewhat larger pressure drops than the other 0.5% nanofluids.

For these nanofluids, Fig. 11 further investigates the relationship between the heat transfer coefficient and the needed pumping power. The pumping power (P_p) is calculated by:

$$P_p = \Delta pV \tag{19}$$

where V is the volume flow rate of the working fluid. It is found that the 1.0 wt.% Al_2O_3-water nanofluid shows the best heat transfer performance at a small pumping power (nearly below 0.4), whereas the 1.0 wt.% Fe_3O_4-water nanofluid shows the best performance at a high pumping power (nearly above 0.5). This result indicates that the nanofluid with the best heat transfer performance should be chosen according to the working conditions in heat transfer systems.

3.4. Empirical formulas

For different nanofluids, the Reynolds number at a given flow rate is different due to the differences in physical properties. In this work, the Reynolds number is calculated by the volume flow rate, dimension of the channel, and physical properties of the heat transfer fluids. Usually, the HTC for fluids in plate heat exchanger can be predicted by the Nusselt number (as a function of Prandtl number and Reynolds number), which is expressed as follows:

$$Nu = CRe^m Pr^n \tag{20}$$

Based on the determination method of the index n in Huang et al. [28], the value of n is classified as a constant of 0.3. The values of C and m are determined by the experimental data. Eq. (21) can be transformed as

$$\lg \frac{Nu}{Pr^{0.3}} = \lg C + m \lg \mathrm{Re} \tag{21}$$

For a nanofluid with a certain concentration, the value of the Prandtl number is a constant. The empirical formula of cold water flowing in the heat exchanger is as follows:

$$Nu = 0.372 Re^{0.687} Pr^{0.3} \tag{22}$$

where the ranges of the Re and Pr are 100–600 and 5–7, respectively. For the 0.05 wt.% Fe_3O_4-water nanofluid, other Nu empirical correlations for plate heat exchangers (Huang et al. [28], Bhattad et al. [29] and Maré et al. [40]) are also shown and listed in Table 6.

Comparisons of experimental and calculated Nu values have been conducted and are shown in Fig. 12. The empirical formula is proposed based on experimental data of water, which was examined using the 0.05 wt.% Fe_3O_4-water nanofluid. From Fig. 10, it is found that the empirical correlation proposed in this work provides predictions agreeing well with experimental results. The maximum error between experimental data and theoretical cal-

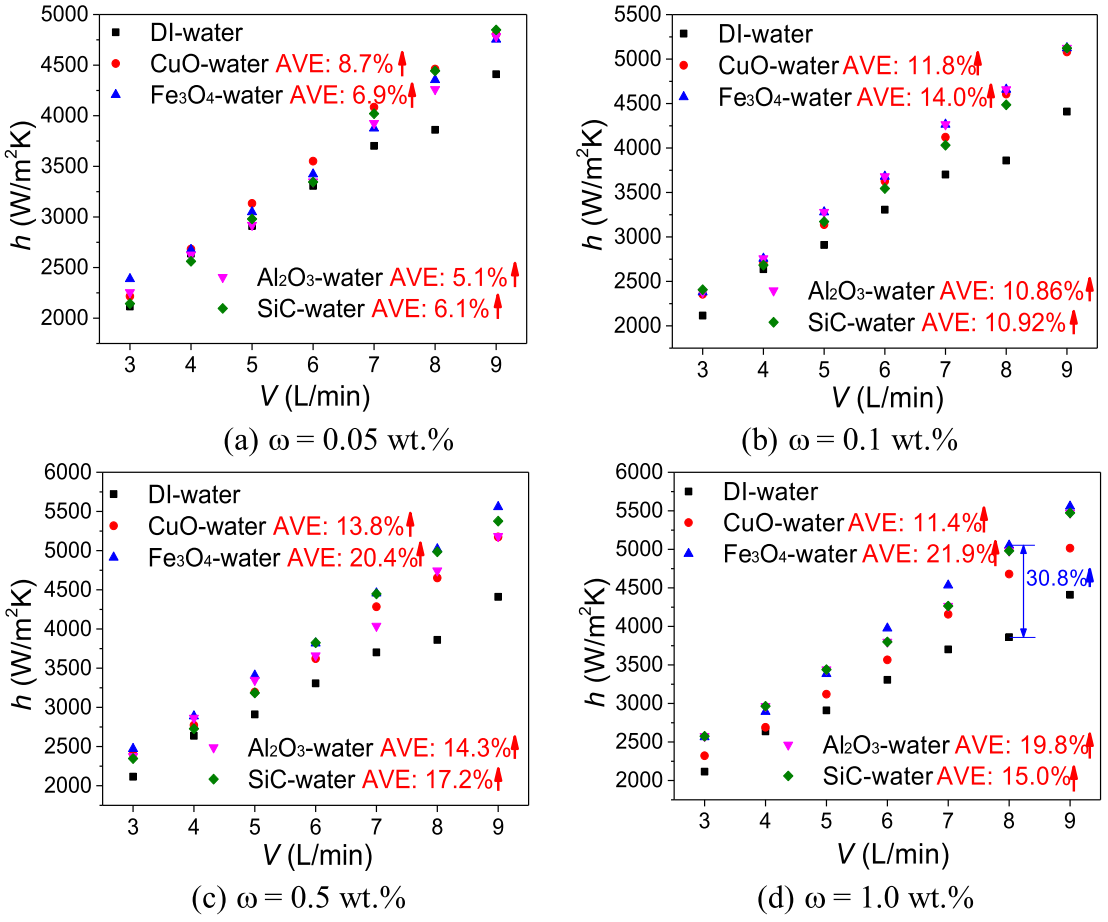

Fig. 9. Heat transfer coefficients of nanofluids for different particle concentrations.

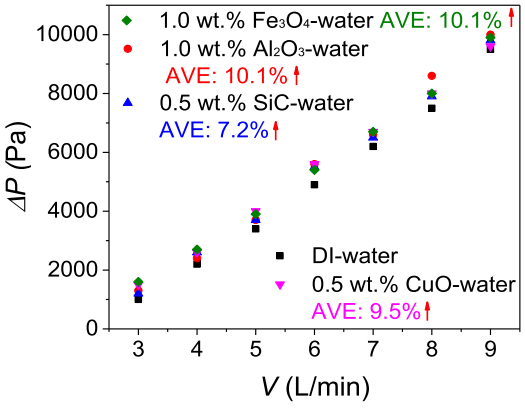

Fig. 10. Pressure drops of various nanofluids.

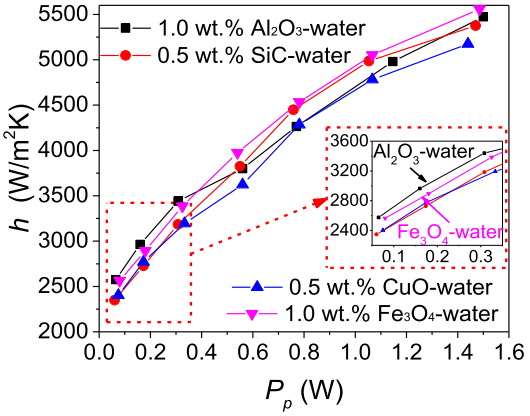

Fig. 11. Heat transfer coefficient of nanofluid with pumping power.

culations is 9.5% at the flow rate of 3 L/min. The average margin of the errors is 2.8% in the whole flow range. If the maximum error at 3 L/min is not considered, the average error decreases to 1.7%. It is found that the deviations are 6.2% and 9.3% from the empirical correlations proposed by Huang et al. [28] and Maré et al. [40], respectively. However, by using the empirical correlation proposed by Bhattad et al. [29], the *Nu* values show great deviations from the experimental values. Different dimensions of

Table 6
Existing heat transfer correlations used in plate heat exchangers.

Authors	Correlations
This study	$Nu=0.372Re^{0.687}Pr^{0.3}$
Huang et al. [28]	$Nu=0.3762Re^{0.6681}Pr^{0.4}$
Bhattad et al. [29]	$Nu=0.358Re^{0.57}Pr^{0.3}$
Maré et al. [40]	$Nu=0.455Re^{0.66}Pr^{1/3}$

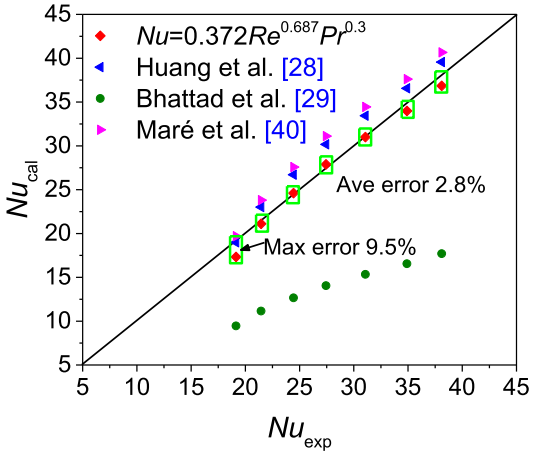

Fig. 12. Comparison between theoretical and experimental *Nu* values for the Fe_3O_4 nanofluid.

plate heat exchangers may cause a difference in the empirical correlations, such as different corrugation angle, corrugation pitch, plate depth, etc.

4. Conclusions

This paper investigated heat transfer performance and flow characteristics of various nanofluids in a corrugated plate heat exchanger used in solar energy systems. Comparisons of heat transfer enhancements of CuO-water, SiC-water, Al_2O_3-water and Fe_3O_4-water nanofluids were conducted at mass flow rates in the range of 3–9 L/min. The main conclusions are as follows:

(1) Compared with DI-water, four nanofluids significantly improve the heat transfer performance of the plate heat exchanger. The Fe_3O_4-water nanofluid at mass fractions above 0.05 wt.% shows higher performance than the other nanofluids. By using 1.0 wt.% Fe_3O_4-water nanofluid as the working fluid, the heat transfer coefficient increases by 30.8% at 8 L/min compared to DI-water.

(2) The pressure drops between the inlet and outlet of the plate heat exchanger were investigated for four nanofluids at the optimum particle concentration. For a given pumping power, the 1.0 wt.% Al_2O_3-water and Fe_3O_4-water nanofluids show higher pressure drop than the other 0.5 wt.% nanofluids especially at high volume flow rates.

(3) The empirical formula of the Nusselt numbers for the tested plate heat exchanger is summarized based on the experimental data. The empirical formula can also provide a reference for application of nanofluids in various heat transfer systems. It is concluded that Fe_3O_4-water nanofluid is a promising medium to enhance the thermal performance of heat transfer systems compared to the other tested nanofluids.

Credit author statement

On behalf of all co-authors, I confirm that all co-authors have significantly contributed to the work reported in this manuscript.

The main work has been carried out by students at Hebei University of Technology (HUT), Tianjin under the initiative, leadership and supervision of Professor Jin Wang. Dr. Jakov Baleta is an external advisor and cooperates with HUT. Professor Bengt Sunden is an external supervisor and advisor. He has long lasting cooperation with Professor Jin Wang. All co-authors contributed significantly to make this study successful. The writing and finalizing of the manuscript are joint work.

On behalf of all co-authors, I confirm that there are no other persons who satisfied the criteria for authorship but are not listed. I further confirm that the order of authors listed in the manuscript has been approved by all co-authors.

Declaration of Competing Interest

On behalf of all co-authors, I wish to confirm that there are no known conflicts of interest associated with this publication and there has been no significant financial support for this work that could have influenced its outcome. I confirm that the manuscript has been read and approved by all named authors and that there are no other persons who satisfied the criteria for authorship but are not listed. I further confirm that the order of authors listed in the manuscript has been approved by all of us.

Acknowledgement

This work is supported by the National Natural Science Foundation of China [Grant numbers 51876161] and Project of Innovation Ability Training for Postgraduate Students of Education Department of Hebei Province [Grant number CXZZSS2019012].

References

[1] M.H. Ahmadi, A. Mirlohi, M. Alhuyi Nazari, R. Ghasempour, A review of thermal conductivity of various nanofluids, J. Mol. Liq. 265 (2018) 181–188.
[2] A. Wahab, A. Hassan, M.A. Qasim, H.M. Ali, H. Babar, M.U. Sajid, Solar energy systems – potential of nanofluids, J. Mol. Liq. (2019) 289.
[3] T.R. Shah, H.M. Ali, Applications of hybrid nanofluids in solar energy, practical limitations and challenges: a critical review, Sol. Energy 183 (2019) 173–203.
[4] J.J. Michael, S. Iniyan, Performance analysis of a copper sheet laminated photovoltaic thermal collector using copper oxide-water nanofluid, Sol. Energy 119 (2015) 439–451.
[5] W. Chen, C. Zou, X. Li, Application of large-scale prepared MWCNTs nanofluids in solar energy system as volumetric solar absorber, Sol. Energy Mater. Sol. Cells 200 (2019) 109931.
[6] A. Yurddaş, Optimization and thermal performance of evacuated tube solar collector with various nanofluids, Int. J. Heat Mass Transf. 152 (2020) 119496.
[7] N. Abbas, M.B. Awan, M. Amer, S.M. Ammar, U. Sajjad, H.M. Ali, N. Zahra, M. Hussain, M.A. Badshah, A.T. Jafry, Applications of nanofluids in photovoltaic thermal systems: a review of recent advances, Phys. A Stat. Mech. Its Appl. 536 (2019) 122513.
[8] A. Radwan, M. Ahmed, Thermal management of concentrator photovoltaic systems using microchannel heat sink with nanofluids, Sol. Energy 171 (2018) 229–246.
[9] M. Mercan, A. Yurddaş, Numerical analysis of evacuated tube solar collectors using nanofluids, Sol. Energy 191 (2019) 167–179.
[10] X. Xu, C. Xu, J. Liu, X. Fang, Z. Zhang, A direct absorption solar collector based on a water-ethylene glycol based nanofluid with anti-freeze property and excellent dispersion stability, Renew. Energy 133 (2019) 760–769.
[11] S. Hashimoto, K. Kurazono, T. Yamauchi, Anomalous enhancement of convective heat transfer with dispersed SiO_2 particles in ethylene glycol/water nanofluid, Int. J. Heat Mass Transf. (2020) 150.
[12] S. Choudhary, A. Sachdeva, P. Kumar, Influence of stable zinc oxide nano fluid on thermal characteristics of flat plate solar collector, Renew. Energy 152 (2020) 1160–1170.
[13] Z. Chen, D. Zheng, J. Wang, L. Chen, B. Sunden, Experimental investigation on heat transfer characteristics of various nanofluids in an indoor electric heater Renew, Energy. (2020) 147.
[14] J. Wang, G. Li, H. Zhu, J. Luo, B. Sundén, Experimental investigation on convective heat transfer of ferrofluids inside a pipe under various magnet orientations, Int. J. Heat Mass Transf. 132 (2019) 407–419.
[15] Z. Said, M. El Haj Assad, A.A. Hachicha, E. Bellos, M.A. Abdelkareem, D.Z. Alazaizeh, B.A.A. Yousef, Enhancing the performance of automotive radiators using nanofluids, Renew. Sustain. Energy Rev. 112 (2019) 183–194.
[16] S. Devireddy, C.S.R. Mekala, V.R. Veeredhi, Improving the cooling performance of automobile radiator with ethylene glycol water based TiO_2 nanofluids, Int. Commun. Heat Mass Transf. 78 (2016) 121–126.
[17] F.C. Nagarajan, S.K. Kannaiyan, C. Boobalan, Intensification of heat transfer rate using alumina-silica nanocoolant, Int. J. Heat Mass Transf. (2020) 149.
[18] M.H. Al-Rashed, G. Dzido, M. Korpyś, J. Smołka, J. Wójcik, Investigation on the CPU nanofluid cooling, Microelectron. Reliab. 63 (2016) 159–165.
[19] P.C. Mukesh Kumar, C.M. Arun Kumar, Numerical study on heat transfer performance using Al_2O3/water nanofluids in six circular channel heat sink for electronic chip, Mater. Today Proc. (2019).
[20] A. Hajatzadeh Pordanjani, S. Aghakhani, M. Afrand, B. Mahmoudi, O. Mahian, S. Wongwises, An updated review on application of nanofluids in heat exchangers for saving energy, Energy Convers. Manage. 198 (2019) 111886.

[21] B.A.K. Naik, A.V. Vinod, Heat transfer enhancement using non-Newtonian nanofluids in a shell and helical coil heat exchanger, Exp. Therm. Fluid Sci. 90 (2018) 132–142.
[22] Z.X. Li, U. Khaled, A.A.A.A. Al-Rashed, M. Goodarzi, M.M. Sarafraz, R. Meer, Heat transfer evaluation of a micro heat exchanger cooling with spherical carbon-acetone nanofluid, Int. J. Heat Mass Transf. (2020) 149.
[23] C. Qi, T. Luo, M. Liu, F. Fan, Y. Yan, Experimental study on the flow and heat transfer characteristics of nanofluids in double-tube heat exchangers based on thermal efficiency assessment, Energy Convers. Manage. 197 (2019) 111877.
[24] N. Mazaheri, M. Bahiraei, H. Abdi Chaghakaboodi, H. Moayedi, Analyzing performance of a ribbed triple-tube heat exchanger operated with graphene nanoplatelets nanofluid based on entropy generation and exergy destruction, Int. Commun. Heat Mass Transf. 107 (2019) 55–67.
[25] P.C. Mukesh Kumar, M. Chandrasekar, CFD analysis on heat and flow characteristics of double helically coiled tube heat exchanger handling MWCNT/water nanofluids, Heliyon 5 (2019) e02030.
[26] R.N. Radkar, B.A. Bhanvase, D.P. Barai, S.H. Sonawane, Intensified convective heat transfer using ZnO nanofluids in heat exchanger with helical coiled geometry at constant wall temperature, Mater. Sci. Energy Technol. 2 (2019) 161–170.
[27] V. Bianco, F. Scarpa, L.A. Tagliafico, Numerical analysis of the Al_2O3-water nanofluid forced laminar convection in an asymmetric heated channel for application in flat plate PV/T collector, Renew. Energy 116 (2018) 9–21.
[28] D. Huang, Z. Wu, B. Sunden, Effects of hybrid nanofluid mixture in plate heat exchangers, Exp. Therm. Fluid Sci. 72 (2016) 190–196.
[29] A. Bhattad, J. Sarkar, P. Ghosh, Experimentation on effect of particle ratio on hydrothermal performance of plate heat exchanger using hybrid nanofluid, Appl. Therm. Eng. 162 (2019) 114309.
[30] M. Shirzad, S.S.M. Ajarostaghi, M.A. Delavar, K. Sedighi, Improve the thermal performance of the pillow plate heat exchanger by using nanofluid: numerical simulation, Adv. Powder Technol. 30 (2019) 1356–1365.
[31] H. Martin, A theoretical approach to predict the performance of Chevron-type plate heat exchangers, Chem. Eng. Process. 35 (1996) 301–310.
[32] B.C. Pak, Y.I. Cho, Hydrodynamic and heat transfer study of dispersed fluids with submicron metallic oxide particles, Exp. Heat Transf. 11 (1998) 151–170.
[33] Y.M. Xuan, W. Roetzel, Conceptions for heat transfer correlation of nanofluids, Int. J. Heat Mass Transf. 43 (2000) 3701–3707.
[34] J.C. Maxwell, A Treatise on Electricity and Magnetism, 2, Longmans, Green, and Co., 2014.
[35] D. Bruggeman, Dielectric constant and conductivity of mixtures of isotropic materials, Ann. Phys. (Leipzig) 24 (1935) 636–679.
[36] A. Einstein, A new determination of molecular dimensions, Ann. Phys. 19 (1906) 289–306.
[37] H.C. Brinkman, The viscosity of concentrated suspensions and solutions, J. Chem. Phys. 20 (4) (1952) 571.
[38] J. Wang, G. Li, T. Li, M. Zeng, B. Sundén, Effect of various surfactants on stability and thermophysical properties of nanofluids, J. Therm. Anal. Calorim. (2020).
[39] R.J. Moffat, Describing the uncertainties in experimental results, Exp. Therm. Fluid Sci. 1 (1988) 3–17.
[40] T. Maré, S. Halelfadl, O. Sow, P. Estellé, S. Duret, F. Bazantay, Comparison of the thermal performances of two nanofluids at low temperature in a plate heat exchanger, Exp. Therm. Fluid Sci. 35 (2011) 1535–1543.